PERIODICA POLYTECHNICA SER. TRANSP. ENG. VOL. 29, NO. 1-2, PP. 83–100 (2001)

ROBUST CONTROL AND FAULT DETECTION FILTER DESIGN FOR AIRCRAFT PITCH AXIS

István SZÁSZI and Balázs KULCSÁR

Department of Control and Transport Automation
Budapest University of Technology and Economics
H–1111 Budapest, Bertalan L. u. 2., Hungary
Phone: +36 14633089, Fax: +36 14633087
e-mail: szaszi@kaut.kka.bme.hu, kulcsar@kaut.kka.bme.hu

Received: October 5, 2001

Abstract

This paper presents a robust control and fault detection filter design for linearized longitudinal dynamics of F-16 aircraft. The control design is based on μ synthesis method which guarantees the robust performance requirements and takes the structured uncertainty into consideration. In case of F-16 aircraft, it is assumed that an elevator failure and a sensor failure occur during the system operation. To ensure the safety of aircraft control system a fault detection and isolation (FDI) filter is designed. The fault detection filter design based on geometric approach relies on the use of (C, A) invariant subspaces which makes possible the decoupling of different types of failure. Typically, the FDI filter design approach is elaborated for open loop model and it is applied in the closed loop. In this paper the FDI filter designed for aircraft control system will be analyzed for a closed loop system.

Keywords: aircraft control, $\mathcal{H}_\infty/\mu$ synthesis, fault detection

1. Introduction

The evolution of modern aircraft created a need for power-driven aerodynamic control surface and automatic pilot control system. In addition, the widening performance envelope created a need to augment the stability of the aircraft dynamics over some parts of the envelope. In case of high performance military aircraft, where the pilot may have to manoeuvre the aircraft to its performance limits and perform tasks such as precision tracking of targets, specialized flight control system is needed. Although the role of a fighter aircraft has changed to include launching missiles from long range, the importance of the classical dogfight is still recognized. Hence in this situation a suitable controlled variable for a pitch axis control system is used as a pitch rate command system. When a situation requires precision tracking of a target, by means of sighting device, it has been found that a pitch rate command is well suited to the task. Systems have been designed [19] which blend together the control of pitch rate and normal acceleration. The experience shows that it is extremely difficult for a pilot to fine track a noncooperative air-to-air target using a system with significant pitch rate overshoot. The flight test experience has shown that the pilots prefer a system with a fast deadbeat pitch rate response for fine tracking.

Traditionally, classical control design based on single-input, single-output techniques has been used to design the flight control system. The classical design approach is aided by such tools as root locus, Bode and Nyquist plots, which enables us to visualize how the system dynamics are being modified, however, the design procedure becomes increasingly difficult as more loops are added [16]. These methods do not guarantee success when the aircraft model contains some uncertainty components or the aircraft dynamics are uncertain. Often, a low order, nominal model, which describes the low-middle frequency range behavior of the plant is available, but the high-frequency plant behavior is uncertain. Recently, the complex μ synthesis has become widespread, because this method yields a compensator that achieves nominal performance and robust stability and takes structured uncertainties into consideration, [4, 5, 15].

In many applications the use of a reliable control system is necessary. It is possible to increase the safety of aircraft with detection of failures in the control loop. The fault detection and isolation problem can be characterized as a two step procedure. The first step is to design a residual generator that produces a signal which is zero or close to zero when no failure is present, but it is different from zero when a component of the system fails. The residuals are examined and a decision rule is then applied to determine if any faults have occurred. The next step is the isolation of the fault by using a special logic to evaluate the situation.

There are various approaches to residual generation, see e.g., the geometric approach to design detection filters as initiated by MASSOUMNIA for LTI systems [11] and used also by BOKOR et al., for LTV systems [6]. The geometric approach relies on the use of (C, A) invariant subspaces and provides conditions on separability (in the detector output error space) and mutual detectability of the failures. The assignment of the effect of a particular fault to a (C, A) invariant subspace of an observer can be solved by using (C, A) invariant subspace algorithm or eigenstructure assignment. The unknown input observer concept is used to fault detection filter design in [2]. The inversion based approach for LTI systems that can be used for detector design is represented as minimum order stable linear system [18]. A complete analysis of the combined feedback controller and fault detection filter has been given in [14, 17] for both nominal systems as well as for uncertain systems. It has been shown that there is a complete separation between the design of feedback controller and FDI filter in the nominal case which is not the case in uncertain systems.

This paper is organized as follows. Section 2 describes the F-16 fighter aircraft nonlinear equations of motion. Section 3 discusses the robust control design based on the μ synthesis. Section 4 gives a very quick review of the fault detection problem. Section 5 demonstrates the F-16 aircraft controller and FDI filter design. A conclusion is given in Section 6.

2. Equations of Motion

In this section the nonlinear longitudinal model of F-16 aircraft is presented. An accurate representation of the dynamics of an aircraft can be obtained through nonlinear, rigid body equations (note that in this case the flexible modes are ignored). References [10, 16], have complete derivations of the rigid body equations for an airplane. The equations of motion of an aircraft can be separated in two parts. One of them includes the translational equations and the other one the rotational equations, respectively. For an aircraft model the rotational motion includes the yawing, pitching and rolling motion, and the three translation motions of the center of gravity (cg). Thus the aircraft model will be a six degrees of freedom mechanical system. The nonlinear equations of motion of a rigid body aircraft could be decoupled into two independent sets of variables. One set of them describes the longitudinal (pitching, and translation in the symmetric plane of the aircraft) motion, and the other set determines the lateral (rolling, and sideslipping and yawing) motion. Under the conditions of small perturbations from steady state flight, the longitudinal aircraft equations of motion could be split into two sets. These are the short period mode that is characterized by change in angle of attack α and pitch attitude θ assuming there is no speed variation and the long period mode or phugoid that is characterized by change of potential and kinetic energy about the equilibrium altitude and speed. The short period mode is heavily damped and it has very short duration. In case of long period, the variation of the angle of attack α is neglected and this motion is a lightly damped mode and it has long duration.

The longitudinal motion of the F-16 can be defined by the following variables: total velocity V_T, angle of attack α, pitch rate q, pitch angle θ. Noting that in longitudinal motion the sideslip angle β, roll angle ϕ, roll p and yaw r rates are considered to be zero. The nonlinear equations for longitudinal motion of F-16 are given by:

$$\dot{V}_T = \frac{1}{m}[F_x \cos\alpha + F_z \sin\alpha], \tag{1}$$

$$\dot{\alpha} = \frac{-F_x \sin\alpha + F_z \cos\alpha + m V_T q}{m V_T + C_{L_{\dot{\alpha}}} \bar{q} S \frac{\bar{c}}{V_T}}, \tag{2}$$

$$\dot{q} = \frac{1}{I_{yy}} M_y, \tag{3}$$

$$\dot{\theta} = q. \tag{4}$$

where m is the aircraft mass and I_{yy} is the mass inertia.

The longitudinal model is affected only by aerodynamic forces along the x and z axis, plus the pitching moment around the y axis. The aerodynamic forces and moments are modelled in terms of aero-coefficients (C_D, C_L, C_m), which can be obtained from wind-tunnel experiments. D denotes the drag, L the lift force and m the pitch moment, respectively. The aerodynamic coefficients are provided as look-up tables function of a wide set of parameters (angle of attack, true airspeed, sideslip angle, altitude and others). The force and moments in body axes are given by:

$$F_x = \bar{q}SC_D + D_T - mg\sin\theta, \tag{5}$$
$$F_z = \bar{q}SC_L + L_T + mg\cos\theta, \tag{6}$$
$$M_y = \bar{q}S\bar{c}\left[C_m + \frac{1}{\bar{c}}(C_L x_{cg} - C_D z_{cg}) + \frac{\bar{c}\dot{\alpha}}{V_T}(C_{m_{\dot{\alpha}}} + \frac{\bar{x}_{cg}}{\bar{c}}C_{L_{\dot{\alpha}}}\right] + M_{Y_T}, \tag{7}$$

where $\bar{q} = \frac{1}{2}\rho V_T^2$ is the dynamic pressure and is a function of Mach number M and altitude h. S is the reference area, $\bar{c}$ is the wing chord and $\bar{x}_{cg}$, $\bar{z}_{cg}$ distances are a measure of the possible moment arms. D_T and L_T are the thrust forces. $C_{L_{\dot{\alpha}}}$ and $C_{m_{\dot{\alpha}}}$ mean the change in lift force and pitching moment coefficient due to the rate of change of angle of attack.

The linear equations of motion needed for control system design will in general be derived by numerical methods from the nonlinear equations. The most widespread methodology to linearize nonlinear systems is the Jacobian linearization. It can be used to create a linear system with respect to an equilibrium point. There is a downside due to the first order approximation used to obtain the linear system. The first order approximation is only acceptable within a small deviation of the trim point. This could lead to divergent behavior with respect to the nonlinear model, for large control inputs. In the linear equations the nonlinear aerodynamic coefficients are replaced by stability derivatives. The stability derivatives are partial derivatives of aerodynamic coefficients with respect to the state variables.

A straight and level flight steady state trim is defined for a nonlinear F-16 aircraft model to get the linearized equations of motion by the Jacobian method. The linearized longitudinal equations are simple, ordinary linear differential equations with constant stability coefficients. The coefficients in the differential equations are made up of aerodynamic stability derivatives, mass and inertia characteristics of the aircraft. The model of longitudinal dynamics in linearized state space form is given by [16]:

$$\dot{x} = Ax + Bu, \tag{8a}$$
$$y = Cx + Dy, \tag{8b}$$

where

$$x = \begin{bmatrix}\dot{V}_T & \dot{\alpha} & \dot{\theta} & \dot{q}\end{bmatrix}^T, \quad u = \delta_{el}, \quad y = \begin{bmatrix}\alpha & q & a_n\end{bmatrix}^T. \tag{9}$$

The states are velocity V_T [ft/sec], the angle of attack α [rad], the pitch angle θ [rad], the pitch rate q [rad/sec]. The control input is elevator deflection δ_{el} [deg]. The outputs are angle of attack α [deg], pitch rate q [deg/sec], and the normal acceleration a_n [g].

3. Robust Servo Control Design Using Complex μ Synthesis

Consider the closed-loop system which includes the feedback structure of the model G_0 and controller K, and elements associated with the uncertainty models and performance objectives (*Fig. 1*). In the diagram, r is the reference, u is the control input, y is the output, n is the measurement noise, and z_e is the deviation of the output from the required one. The structure of the controller K may be partitioned into two parts: $K = \begin{bmatrix} K_r & K_y \end{bmatrix}$, where K_y is the feedback part of the controller and K_r is the pre-filter part.

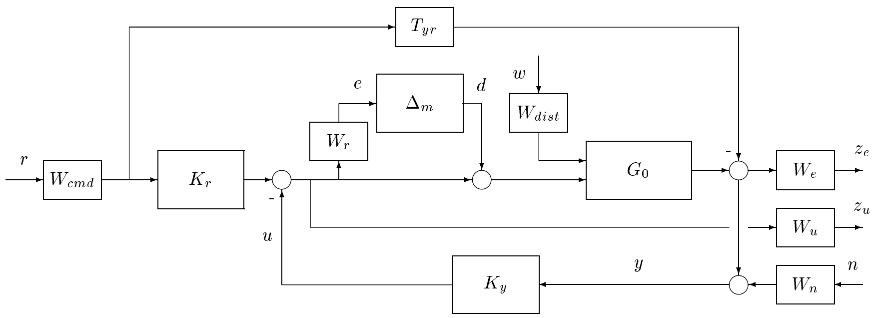

Fig. 1. Closed loop interconnection structure

Often, a low order, nominal model, which describes the low-middle frequency range behavior of the plant is available, but the high-frequency plant behavior is uncertain. In this situation, even the dynamic order of the actual plant is not known, and something richer than parametric uncertainty is needed to represent the unmodeled dynamics. One common approach for this type of uncertainty is to use a multiplicative uncertainty model. Roughly, this allows you to specify a frequency-dependent percentage uncertainty in the actual plant behavior. In our case an input multiplicative uncertainty is used. The uncertainties between the nominal model and the real plant is represented by W_r and Δ_m. W_r is assumed to be known, and it presents all a priori information about the neglected dynamics. The transfer function Δ_m is assumed to be stable and unknown with the norm condition, $\|\Delta_m\|_\infty < 1$. The precise definition of the multiplicative uncertainty is as follows:

$$M(G_0, W_r) := \left\{ G : \left| \frac{G(i\omega) - G_0(i\omega)}{G_0(i\omega)} \right| \le |W_r(i\omega)| \right\}. \tag{10}$$

At each frequency, $|W_r(iw)|$ represents the maximum potential percentage difference between all of the plants represented by $M(G_0, W_r)$ and the nominal plant model G_0. In that sense, $M(G_0, W_r)$ represents a ball of possible plants, centered at G_0. On a Nyquist plot, a disk of radius $|W_r(iw)G_0(iw)|$, centered at $G_0(iw)$ is the set of possible values that it can take on, due to the uncertainty description. Design models used for flight control typically exhibit good fidelity at lower frequencies, say $\omega < 10-20$ rad/sec, but they degrade rapidly at higher frequencies due to such poorly modelled or neglected effects as aeroelasticity, actuator modelling error, and so on. Such modelling errors are well-represented by complex-valued, unstructured, multiplicative perturbations located at plant input.The complex-valued unstructured representation is appropriate here because magnitude and phase errors and cross channel coupling errors are all prominent at higher frequencies. The multiplicative form is chosen for convenience because it permits the intuitive interpretation of uncertainty magnitudes in terms of percent errors relative to the design model.

The weighting function W_e chosen for tracking errors can be thought of as penalty function. That is, weights should be large in the frequency range where small errors are desired and small where larger errors can be tolerated. The size and frequency response shapes of tracking error weights depend upon several considerations. First, we should recognize that the errors at frequencies beyond feedback loop bandwidth will necessarily be open loop size. Second, to achieve integral action (i.e. zero steady state errors), weights should be large at very low frequency. When choosing tracking performance weights for design tradeoffs, it is also important to keep in mind the range of validity of the design model. For instance, there is nothing to be gained by requiring integral action for an error signal when the design model does not correctly represent low frequency characteristics. The short period approximation of longitudinal aircraft dynamics, which neglects phugoid modes, is a case in point. T_{id} is the model matching function which generally is an ideal transfer function of the plant. The performance objective of the two degree of freedom controller design is the $\left\| T_{z_e r} \right\|_\infty$ to be small for all possible $\|\Delta_m\|_\infty < 1$.

The control inputs are limited using a performance criterion W_u. Using this weight the designer can penalize larger deflections and thereby minimize control activity. The simplest weight on actuator deflection is constant across frequency and has a magnitude equal to the inverse of the deflection.

Now, let us consider the role of weights for external disturbance signals. Recall that these signals include sensor noise W_n, external disturbances W_{dist} and pilot commands W_{cmd}. The role of weights for these signals is basically the opposite of the role of weights for output weights discussed so far. Inputs to the weights are signals whose frequency responses are flat and unit size. The weights themselves contain scale factors and frequency shaping that match the size, units and frequency content of the true inputs. Typically we have only two categories of disturbance weights. The first category consists of simple constants that are used to model wide band signals such as sensor noise W_n. In most flight control designs, sensor noises are small and do not affect performance significantly. The second category of disturbance weights consists of low pass filters that are used to model band limited signals such as gusts W_{dist} and pilot commands W_{cmd}. Typically these weights are first order transfer functions with gains selected to produce the correct signal levels and time constants selected to match the bandwidth of the signals.

Necessary and sufficient conditions for robust stability and robust performance can be formulated in terms of the structured singular value denoted as μ [4].

Now, the design setup in *Fig. 1* should be formalized as a standard design problem as illustrated in *Fig. 2*.

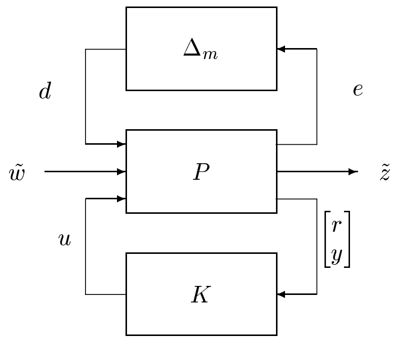

Fig. 2. Generalized $P - K$ structure

By applying the weighting functions and the compensator, the augmented plant P can be formalized as *Eq.* (11).

$$\begin{bmatrix} e \\ z_e \\ z_u \\ \hline r \\ y \end{bmatrix} = \left[\begin{array}{cccc|c} 0 & 0 & 0 & 0 & W_r \\ W_e G_0^u & -W_e T_{id} & 0 & W_e G_0^w & W_p G_0^u \\ 0 & 0 & 0 & 0 & W_u \\ \hline 0 & I & 0 & 0 & 0 \\ G_0^u & 0 & W_0 & G_0^w & G_0^u \end{array}\right] \begin{bmatrix} d \\ r \\ n \\ w \\ \hline u \end{bmatrix}, \tag{11}$$

where

$$\tilde{w} = \begin{bmatrix} r & n & w \end{bmatrix}^T, \quad \tilde{z} = \begin{bmatrix} z_e & z_u \end{bmatrix}^T. \tag{12}$$

A new matrix function called linear fractional transformation (LFT) is introduced. A lower LFT can be formally defined provided that the inverse $(I - P_{22}K)^{-1}$ exists:

$$F_l(P, K) := P_{11} + P_{12}K(I - P_{22}K)^{-1}P_{21}. \tag{13}$$

In order to analyze the performance and robustness requirements, the closed loop system is expressed by the lower linear fractional transformation:

$$M = P_{11} + P_{12}K(I - P_{22}K)^{-1}P_{21}, \tag{14}$$

$$\begin{bmatrix} e \\ \hline \tilde{z} \end{bmatrix} = \left[\begin{array}{c|c} M_{11} & M_{12} \\ \hline M_{21} & M_{22} \end{array}\right] \begin{bmatrix} d \\ \hline \tilde{w} \end{bmatrix}. \tag{15}$$

Assume that Δ_m is a member of the bounded subset:

$$\mathbf{B}\Delta = \{\Delta_m \in \Delta \,|\, \overline{\sigma}\{\Delta\}_m < 1\}, \tag{16}$$

where Δ is defined by:

$$\boldsymbol{\Delta} = \{\text{diag}(\delta_1^c I_{r_1}, \cdots, \delta_{m_c}^c I_{r_{m_c}}, \Delta_1, \cdots, \Delta_n) \mid \delta_i^c \in \mathbb{C}, \Delta_j \in \mathbb{C}^{m_j \times m_j}\}. \tag{17}$$

where the ith repeated complex scalar block is $r_i \times r_i$, and the jth full block is $m_j \times m_j$.

The robust stability (RS) can be guaranteed when the closed-loop system is internally stable. The internal stability means that from all inputs to all outputs the created transfer function is stable. Robust stability is equivalent to:

$$\|M_{11}\|_\infty < 1. \tag{18}$$

We restrict the set of perturbation to $\Delta \in \mathbf{B}\boldsymbol{\Delta}$ and therefore condition (18) can be arbitrarily conservative. Rather than a singular value constraint we need some measure which takes into account the structure of the perturbations Δ. This is the structured singular value μ.

The structured singular value can be defined as

$$\mu_\Delta(M) = \frac{1}{\min_\Delta(\overline{\sigma}\{\Delta\} : \ \Delta \in \boldsymbol{\Delta},\ \det(I + \Delta M) = 0)}, \tag{19}$$

unless no $\Delta \in \boldsymbol{\Delta}$ makes $I - M\Delta$ singular, in which case $\mu_\Delta(M) = 0$. Thus $1/\mu_\Delta(M)$ is the "size" of the smallest perturbation Δ, measured by its maximum singular value, which makes $\det(I - M\Delta) = 0$.

From the definition of μ, the robust stability can be reformulated as:

$$\sup_\omega \mu(M_{11}) < 1 \Longleftrightarrow \|\mu(M_{11})\|_\infty < 1. \tag{20}$$

The main goal of our synthesis is to guarantee robust performance (RP). The closed-loop system achieves robust performance if the performance objective is met:

$$\sup_\omega \mu(M) < 1 \Longleftrightarrow \|\mu(M)\|_\infty < 1. \tag{21}$$

Using μ it is possible to test for both robust stability and robust performance in a non-conservative manner.

Unfortunately *Eq.* (19) is not suitable for computing μ since the implied optimization problem may have multiple local maxima. However, tight upper and lower bounds for μ may be effectively computed for complex perturbation sets. Algorithms for computing these bounds have been documented in several papers, see e.g. [5].

Define

$$\mathcal{D} = \left\{ \begin{array}{c} \text{diag}\left[D_1, \ldots, D_{m_c}, d_1 I_{m_1}, \ldots, d_n I_{m_{n-1}}, I_{m_n}\right] : \\ D_i \in \mathbb{C}^{r_i \times r_i}, D_i = D_i^* > 0 \end{array} \right\}. \tag{22}$$

The upper bound can be formulated as a convex optimization problem, so the global minimum can be found. For a constant matrix M and complex uncertainty structure Δ, an upper bound for $\mu_\Delta(M)$ is as follows:

$$\mu_\Delta(M) \leq \inf_{D\in\mathcal{D}} \overline{\sigma}\left\{D^{-1}MD\right\}. \tag{23}$$

The aim of the μ synthesis is to minimize the peak value of $\mu_\Delta(.)$ of the closed-loop M for all stabilizing controllers K.

Using the upper bound the optimization problem can be formulated as:

$$\min_K \sup_\omega \inf_{D(\omega)\in\mathcal{D}} \overline{\sigma}\left\{D^{-1}(\omega)\mathcal{F}_l(P,K)D(\omega)\right\}. \tag{24}$$

Unfortunately, it is not known how to solve (24). However, an approximation to complex μ synthesis can be made by the following iterative scheme. For a fixed controller $K(s)$, the problem of finding $D(\omega)$ is just the complex μ upper bound problem which is a convex problem with known solution. Having found these scalings we may fit stable minimum phase transfer function matrices $D(s)$ to $D(\omega)$ such that the interconnection $D(s)M(s)D(s)^{-1}$ is stable. For given scalings $D(s)$ the problem of finding a controller $K(s)$ which minimizes the norm $\left\|\mathcal{F}_l(D(s)M(s)D^{-1}(s), K(s))\right\|_\infty$ will be reduced to a standard $\mathcal{H}_\infty$ problem. Repeating this procedure, denoted $D-K$ iteration, several times yields the complex μ optimal controller provided the algorithm converges.

4. Detection Filter Problem

Consider a system with additive actuator and sensor fault model:

$$\dot{x} = Ax + Bu + \sum_{i=1}^{k} L_i \nu_i, \tag{25a}$$

$$y = Cx + \sum_{j=1}^{q} e_j \mu_j. \tag{25b}$$

In *Eq.* (25), $x \in \mathcal{X}$ is the state variable, $u \in \mathcal{U}$ is the known control input, $y \in \mathcal{Y}$ is the known output, the arbitrary time-varying functions $\nu_i \in \mathcal{V}$ and $\mu_j \in \mathcal{M}$ are the unknown failure modes. The failure modes are zero when there is no failure. The maps $L_i : \mathcal{V}_i \to \mathcal{X}$ are the failure signatures. A failure mode ν_i models the time varying amplitude of a failure while a failure signature L_i models the directional characteristics of a failure. ν_i can represent the actuator fault. For example, the effect of failure in the ith actuator can be represented by $L_i = B_i$ where B_i is the ith column of B. μ_i can model the sensor fault. e_j are the unit vector. E.g., the effect of failure in the ith sensor can be represented by e_i where the ith element of e_i is the unit element and the other elements of e_i are equal to zero.

Design an observer in the form:

$$\dot{\hat{x}} = A\hat{x} + Bu + D(y - \hat{y}), \quad \hat{x}(0) = x(0), \tag{26a}$$

$$\hat{y} = C\hat{x}. \tag{26b}$$

We refer to $D : \mathcal{Y} \to \mathcal{X}$ as the output injection map or the observer gain matrix. Let the state estimation error be $\epsilon = x - \hat{x}$ and the residual $r = y - C\hat{x}$, respectively. The error system is as follows:

$$\dot{\epsilon} = (A - DC)\epsilon + \sum_{i=1}^{k} L_i \nu_i - d_j \mu_j, \tag{27a}$$

$$r = T\left(C\epsilon + \sum_{j=1}^{q} e_j \mu_j\right), \tag{27b}$$

where d_j is the jth column of the detection filter gain matrix. The presence of d_j in (27a) is a potential difficulty since the detection gain is not known a priori. The objective of the design procedure for a sensor failure is to determine two a priori directions associated with a failure in the jth sensor such that the output errors lie somewhere in the plane defined by Cd_j and e_j. The closed loop error system of (27) can be replaced by a system of the form

$$\dot{\epsilon} = (A - DC)\epsilon + \sum_{i=1}^{k} L_i \nu_i + \sum_{j=1}^{q} l_j^* \mu_j + \sum_{j=1}^{q} l_j \mu_j, \tag{28a}$$

$$r = TC\varepsilon, \tag{28b}$$

where l_j is any direction such that $e_j = Cl_j$ and $l_j^* = Al_j$.

Eq. (28) can be reformulated as follows:

$$\dot{\epsilon} = (A - DC)\epsilon + \sum_{i=1}^{k+q} F_i f_i, \tag{29a}$$

$$r = TC\epsilon, \tag{29b}$$

where f_i contains both ν_i and μ_j failure modes, moreover F_i consists of all failure signatures.

The detection filter problem can be stated in geometric language as follows. Given A, F_i $(i = k + q)$ and C, find a compatible and output separable family of (C, A)-invariant subspaces $\{\mathcal{W}_i, \ i \in k + q\}$ such that $\mathcal{F}_i \subseteq \mathcal{W}_i$. In other words, find $\{\mathcal{W}_i, \ i \in k + q\}$ such that there exists a D with

$$(A - DC)\mathcal{W}_i \subseteq \mathcal{W}_i, \tag{30}$$

$$\mathcal{F}_i \subseteq \mathcal{W}_i, \tag{31}$$

$$C\mathcal{W}_i \cap \sum_{i \neq j} C\mathcal{W}_i = 0. \tag{32}$$

Note that if there exists a family of subspaces $\{\mathcal{W}_i,\ i \in k+q\}$ and an observer gain D such that the conditions in (30) and (31) are satisfied, then the error ϵ due to a nonzero f_i remains inside $\mathcal{W}_i$ which contains the reachable subspace of $(A - DC, F_i)$. Also (32) requires the subspaces $C\mathcal{W}_i$ to be independent so that the residual vector due to the different failures is confined to independent subspaces of the output space. The fault is identified by projecting r onto each of the output subspaces $C\mathcal{W}_i$ using T projection matrix. If the initial error $\epsilon(0)$ is not zero, then naturally we should add a stability requirement (33) to the problem statement so that the initial observation error dies away and the residual stays close to zero when no failure is present.

$$\lambda_i((A - DC)\,|\,\mathcal{W}_i) \quad < \quad 0 \quad \forall i. \tag{33}$$

To ensure stability, instead of the minimal (C, A)-invariant subspaces $\mathcal{W}_i^*$, a set of mutually detectable, minimal unobservability subspaces or detection subspaces $\mathcal{I}_i$ are usually chosen. The $\mathcal{I}_i^*$ the smallest unobservability subspaces (UOS) containing $\mathcal{F}_i$ and the largest UOS in Ker C satisfy the conditions. Moreover, $\mathcal{I}_i^*$ has the additional property that the spectrum of $(A - DC)$ is arbitrarily assignable. $\mathcal{W}_i^*$, and $\mathcal{I}_i^*$ can be computed by *CAISA* and *UOSA* algorithms, respectively [20].

$$CAISA: \quad \begin{cases} \mathcal{W}_0 = 0, \\ \mathcal{W}_{k+1} = \mathcal{F} + A(\mathrm{Ker}C \cap \mathcal{W}_k), \end{cases} \tag{34}$$

$$UOSA: \quad \begin{cases} \mathcal{S}_0 = \mathcal{X}, \\ \mathcal{S}_{k+1} = \mathcal{W}^* + (A^{-1}\mathcal{S}_k) \cap \mathrm{Ker}C. \end{cases} \tag{35}$$

5. $\mathcal{H}_\infty/\mu$ Controller and FDI Filter Design

This section presents the design of a controller for the longitudinal axis F-16 aircraft model using $\mathcal{H}_\infty/\mu$ control technique and an FDI filter based on (C, A) invariant subspace algorithm, respectively.

First, the objective is to design a linear, robust, multivariable controller which achieves good pitch rate command tracking. The aircraft dynamics of F-16 are linearized for a straight and level flight condition at sea level and 0.45 M for a four state model that includes only the longitudinal dynamics.

The state space matrices of the linearized longitudinal motion of F-16 are as follows:

$$A = \begin{bmatrix} -0.0193 & 8.8157 & -32.1700 & -0.5749 \\ -0.0002 & -1.0189 & 0 & 0.0506 \\ 0 & 0 & 0 & 1 \\ 0.0000 & 0.8222 & 0 & -1.0774 \end{bmatrix}, \qquad B = \begin{bmatrix} 0.1737 \\ -0.0021 \\ 0 \\ -0.1755 \end{bmatrix} \tag{36}$$

$$C = \begin{bmatrix} 0 & 57.2957 & 0 & 0 \\ 0 & 0 & 0 & 57.2957 \\ 0.0039 & 15.8800 & 0 & 1.4810 \end{bmatrix}, \qquad D = \begin{bmatrix} 0 \\ 0 \\ 0.0333 \end{bmatrix}. \tag{37}$$

The elevator actuator dynamics is a first order transfer function $G_{el} = \frac{25}{s+25}$.

The sensor models represent the sensor dynamics. The α and q sensors are taken as unity, and a_n sensor is chosen as a second order system:

$$S_\alpha = 1, \tag{38}$$

$$S_q = 1, \tag{39}$$

$$S_{a_n} = \frac{39.27^2}{s^2 + 2 \cdot 0.7 \cdot 39.27s + 39.27^2}. \tag{40}$$

The W_r weight describes model uncertainty at the model input

$$W_r = 2\frac{s+2}{s+20}. \tag{41}$$

This choice indicates in case of elevator uncertainty weight that at frequencies below 2 rad/sec, we expect 20% model error. For frequencies above 2 rad/sec, the model uncertainty grows until the pole at 20 rad/sec, which is needed to make the weighting function realizable. The longitudinal models are generally reliable out to between 2 and 10 rad/sec. But, our weighting function is chosen to indicate that the model loses fidelity beyond 2 rad/sec. By increasing model uncertainty beyond 2 rad/sec, the optimization keeps bandwidth roughly between 2 and 20 rad/sec (see *Fig. 3*).

For this example, optimal performance is measured in terms of model tracking errors. The pilot input is the stick and the reference signal is the pitch rate q.

First, the weighting functions have to be selected for a design method. The W_{cmd} weight takes a unit-norm signal as input and produces a signal with size and frequency content consistent with pilot commands. For example, in a flight control problem, fighter pilots can generate stick input reference commands up to a bandwidth of about 2Hz. Say the stick has a maximum travel of 3 inches. Pilot commands would then be modelled as normalized signals passed through a first order filter:

$$W_{cmd} = 0.001\frac{s+100}{s+0.1}. \tag{42}$$

The W_e transfer function weight is the difference between the idealized q response and the actual aircraft responses

$$W_e = 4\frac{s + 2.5 \cdot 10^{-3}}{(s+0.1) \cdot (s+0.1)}. \tag{43}$$

W_e is chosen in such a way that the short period modes are emphasized for tracking performance. Therefore the weight has a peak in the middle frequency range which is the short period approximation. *Fig. 3* shows the robust (dashed) and tracking performance (solid) weighting functions.

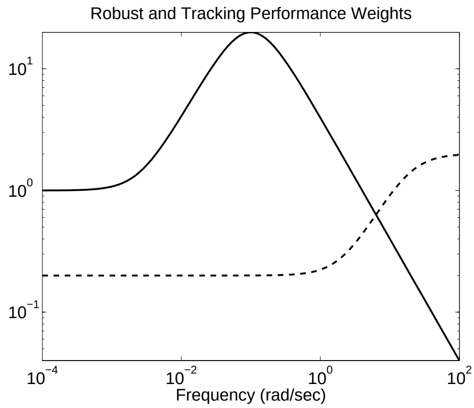

Fig. 3. Robust and tracking weighting functions

T_{id} represents a desired ideal model for the closed-loop system from the pilot stick to output. The ideal response is given by the handling quality (HQ) description. For good command tracking response we might desire our closed-loop system to respond as a first-order system. The model matching function is given by:

$$T_{id} = \frac{2.5}{s + 2.5}. \tag{44}$$

The W_{dist} scales unit norm signals to have proper size and frequency content for disturbance input. For this example the disturbance is a dynamic gust disturbance model, which is evaluated from the formulas and graphs in the MIL-F-8785-C for 0.45 M [12]:

$$W_{dist} = \frac{0.975s + 0.25}{s^2 + 0.88s + 0.19}. \tag{45}$$

The W_u weight is used to shape the penalty on control signal usage. The weights penalize the deflection limits response of the control signal, in the face of the tracking and disturbance rejection objectives already defined. The elevator limit is defined as ± 25 deg for deflection

$$W_u = \frac{1}{25}. \tag{46}$$

W_n represents the frequency content of sensor noise. The weights are derived from laboratory experiments or based on manufacturer measurements. Noises weights are given by:

$$W_n^{\alpha} = 0.1, \tag{47}$$
$$W_n^{q} = 0.1, \tag{48}$$
$$W_n^{a_n} = 0.01g. \tag{49}$$

The sensor noise for α and q channel is 0.1 deg and 0.1 deg/sec, respectively. There is a $0.01g$ measurement noise for the acceleration sensor.

Using the weighting functions of the nominal performance and the robust stability specifications, the optimal $\mathcal{H}_\infty$ controller is designed using the standard gamma iteration. The gamma value achieved is 1.709. The M_{11} and M_{22} transfer functions associated with robust stability and nominal performance may be evaluated separately. The controlled system achieves robust stability, however, it does not achieve nominal performance. This conclusion follows from the singular value plots as it is shown in *Fig. 4(a)*. It is observed that the nominal performance increases above 1 in the low frequency range.

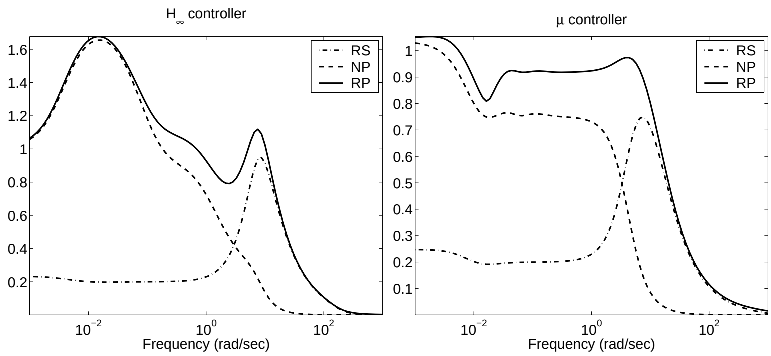

(a) $\mathcal{H}_\infty$ controller case (b) μ controller case

Fig. 4. Robust stability, nominal performance and robust performance

In the next step, the D-K iteration is performed. The results of Step 4 of the D-K iteration are shown in *Fig. 4(b)*.

It is claimed that both the nominal performance and the robust stability requirements are fulfilled. Moreover, robust performance is also achieved, because the value of μ is under 1. The important values of the steps of the D-K iterations are shown in *Table 1*. The controller order is selected 21. No attempt was made to reduce the state order of the controller.

Next an FDI problem is considered for open loop using the geometric approach for fault in elevator actuator and pitch rate sensor fault, respectively [11]. The fault detection filter is studied in linear closed loop simulation, and it is reported to perform well in the presence of sensor noise.

Our system can be described by the following linear time invariant model:

$$\dot{x} = Ax + Bu + b_{el}\nu, \tag{50a}$$

$$y = Cx + e_q\mu. \tag{50b}$$

The actuator failure can be modeled as an additive term in the state equation where

Table 1. Iteration summary

Iteration	#1	#2	#3	#4
Controller order	13	17	19	21
D-scale order	0	4	6	8
Gamma achieved	2.344	1.963	1.380	1.063
Peak μ value	1.419	1.918	1.362	0.974

the failure signature b_{el} is the same as the first column of the B matrix, which represents the elevator actuator direction. The sensor failure can be modeled similarly to actuator fault as an additive term in the measurement equation. The sensor failure signature is a unit vector. The e_q means that the arbitrary time-varying real scalar μ has only effect on the pitch rate sensor. *Eq.* (50) can be reformulated in such form where all faults are modeled only in the state equation. Therefore the sensor failure has to be modeled as a pseudo-actuator failure. As explained in Section 2 the e_q failure signature is equivalent to a two dimensional fault F_q. The modified fault model is as follows:

$$\dot{x} = Ax + Bu + F_\delta \nu + F_q \mu, \tag{51a}$$
$$y = Cx, \tag{51b}$$

where

$$F_\delta = b_{el}, \quad F_q = \begin{bmatrix} F_q^1 & F_q^2 \end{bmatrix} \tag{52}$$

and the directions F_q^1 and F_q^2 are given by

$$e_q = CF_q^1, \quad F_q^2 = AF_q^1. \tag{53}$$

Now let us apply the geometric approach based on (C, A)-invariant concept to (51). Considering the actuator and sensor failure, the error system is given in the following way:

$$\dot{\epsilon} = (A - DC)\,\epsilon + F_\delta \nu + F_q \mu, \tag{54a}$$
$$r = TC\epsilon. \tag{54b}$$

The designed detection filter based on open loop will be applied to closed loop. In case of closed loop analysis the filter inputs are the controlled outputs moreover the controller output which is the elevator deflection δ_e. A 1 deg step actuator failure is simulated occurring at 20 sec and a 0.2 deg/sec doublet sensor failure occurring between 10 sec and 25 sec, respectively. The FDI filter is tested during an aircraft manoeuvre. The responses of 1 deg/sec doublet command in pitch rate are plotted in *Fig. 5*. It is observed that for a 1 deg/sec doublet command in pitch rate, the pitch rate response has a settling time of 2 sec. The effect of the two failures appears only in pitch rate and in normal acceleration, but it dies out with small deviation. The required control inputs can be seen in *Fig. 6*. The elevator deflection is within acceptable limits.

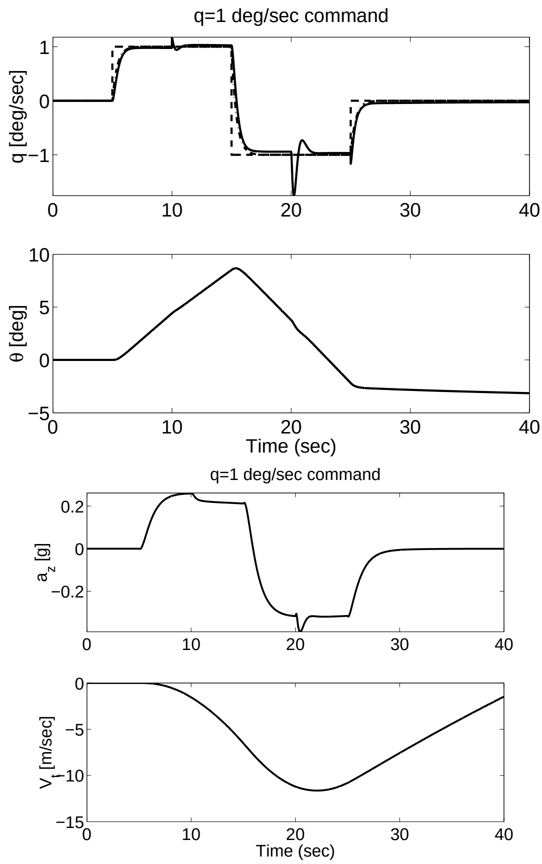

Fig. 5. 1 deg/sec doublet command in pitch rate channel

The simulation result of the FDI filter in case of closed loop can be seen in *Fig. 7*. The first residual shows the actuator fault and the second residual the sensor fault. The two types of failure are decoupled and the residuals give an exact estimation of elevator fault and sensor fault, respectively. The effect of pitch rate command on residuals is negligible.

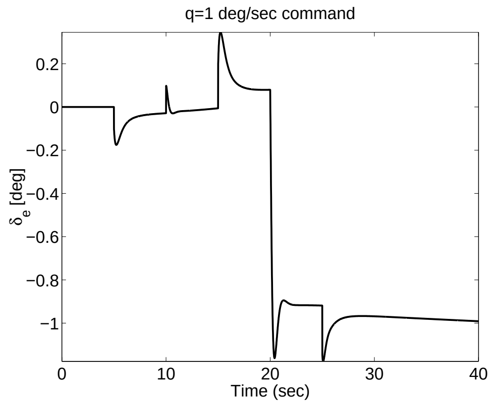

Fig. 6. 1 deg/sec doublet command in pitch rate channel

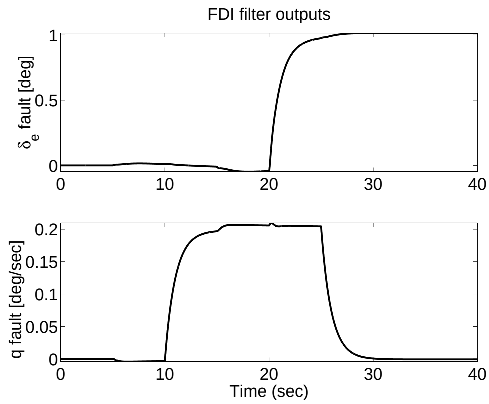

Fig. 7. 1 deg step elevator fault and 0.2 deg/sec doublet sensor fault

6. Conclusion

In this paper, an $\mathcal{H}_\infty/\mu$ control and an FDI filter design based on (C, A) invariant subspace concept has been presented through the application of LTI F-16 longitudinal model. The designed $\mathcal{H}_\infty$ controller fulfils the predefined robust stability requirement, however, it does not fulfil the predefined performance requirement. Applying D-K iteration in the μ synthesis, the designed controller guarantees not only the nominal performance but also the robust performance. The FDI filter design can be independently performed from control design in nominal case. In many cases one designs an FDI filter for open loop and it will be applied to closed loop.

References

[1] BALAS, G. J. – DOYLE, J. C. – GLOVER, K. – PACKARD, A. – SMITH, R., *μ Analysis and Synthesis Toolbox*, MUSYN Inc. and The Mathworks Inc., 1991.

[2] CHEN, J. – PATTON, R. J., *Robust Model based Fault Diagnosis for Dynamic Systems*, Kluwer, Boston/Dordrecht/London, 1999.

[3] CSERE, K. – BOKOR, J., *Detection Filter Design for Twodimensional Failure Signatures*, Technical report, Computer and Automation Research Institute, Hungarian Academy of Sciences, 1989.

[4] DOYLE, J., Structured Uncertainties in Control System Design, *Proc. of the 24th Conference on Decision and Control*, Lauderdale, (1985), pp. 260–265.

[5] DOYLE, J. C. – PACKARD, A., Uncertainty Multivariable Systems from a State Space Perspective, In *Proc. American Control Conf.*, (1987) pp. 2147–2152, Minneapolis, MN.

[6] EDELMAYER, A. – BOKOR, J. – SZIGETI, F. – KEVICZKY, L., Robust Detection Filter Design in the Presence of Time-Varying System Perturbations, *Automatica*, **33** (3) (1997), pp. 471–475.

[7] GANGULI, S. – BALAS, G. J., A TECS Alternative using Robust Multivariable Control, *AIAA Guidance, Navigation, and Control Conference and Exhibit*, Montreal, Canada, (2001), paper no. AIAA 2001–4022.

[8] HANKE, C., The Simulation of a Large Jet Transport Aircraft, *Vol.1: Mathematical Model, Tech. Rep. NASA*, (1971), CR-1756.

[9] HANKE, C. – NORDWALL, D., The Simulation of a Jumbo Jet Transport Aircraft, *Vol.1: Modeling Data, Tech. Rep. NASA*, (1970), CR-114494/D6-30643-VOL-2.

[10] MARCOS, A., A Linear Parameter Varying Model of the Boeing 747-100/200 Longitudinal Motion, *Master's thesis*, Department of Aerospace and Engineering Mechanics, University of Minnesota, 2001.

[11] MASSOUMNIA, M. A., A Geometric Approach to the Synthesis of Failure Detection Filters, *IEEE Trans. Automat. Contr.*, AC-**31 9** (1986), pp. 839–846.

[12] Military Specification Flying Qualities of Piloted Airplanes, *MIL-F-8785C Notice 2*, approved for public release, distribution unlimited, 28 August, 1996.

[13] NELSON, R., Flight Stability and Automatic Control, McGraw-Hill, 1998.

[14] NIEMANN, H. – STOUSTRUP, J., Integration of Control and Fault Detection: Nominal and Robust Design, *Proc. of IFAC Symposium on Fault Detection*, Hull, (1997), pp. 341–346.

[15] PACKARD, A. – DOYLE, J., The Complex Structured Singular Value, *Automatica*, **29** No. 1 (1993), pp. 71–109.

[16] STEVENS, B. L. – LEWIS, F. L., *Aircraft Control and Simulation*, John Wiley and Sons, 1992.

[17] STOUSTRUP, J. – GRIMBLE, M. J., Integration Control and Fault Diagnosis: A Separation Result, *Proc. of IFAC Symposium on Fault Detection*, Hull, (1997), pp. 341–346.

[18] SZIGETI, F. – VERA, C. E. – BOKOR, J. – EDELMAYER, A., Inversion Based Fault Detection and Isolation, *IEEE Conf. on Decision and Control* (2001).

[19] TOLES, R. D., Application of a Digital Multi-Input/Multi-Output Control Law with Command Path Blended Gains for the Pitch Axis Task-Tailored Air Combat Mode of the AFTI/F-16, In *Proc. American Control Conf.*, Boston, (1985), pp. 1475–1480.

[20] WONHAM, W. M., *Linear Multivariable Control – A Geometric Approach*, Springer-Verlag, New York, 1985, (Third Edition).